

PAPER • OPEN ACCESS

The Effect of Boron Addition on the corrosion behavior of Ni Cr Modental alloy prepared by powder metallurgy.

To cite this article: Ali Hubi Haleem *et al* 2021 *J. Phys.: Conf. Ser.* **1973** 012152

View the [article online](#) for updates and enhancements.



ECS **240th ECS Meeting**
Digital Meeting, Oct 10-14, 2021
We are going fully digital!
Attendees register for free!
REGISTER NOW

The banner features a group of diverse professionals in a meeting setting, with a man in a white shirt and tie clapping and a woman in a grey patterned top looking at a tablet. The background is a blurred office environment.

The Effect of Boron Addition on the corrosion behavior of Ni Cr Modental alloy prepared by powder metallurgy.

Ali Hubi Haleem¹, Haydar H.J. Jamal Al-Deen¹, Ban Ahmed shanan²

¹ Department of Metallurgical Engineering, Materials Engineering Faculty, University of Babylon, Iraq. ² MSc. Materials Engineering, University of Babylon, Iraq.

alialihhobi@gmail.com, jaberjd@gmail.com, ban.ahmad79@yahoo.com

Abstract. The powder metallurgy (PM) method was used to create the alloy. The sintering process was carried out in an inert high-temperature tube furnace in the presence of inert gas at a temperature of 1000 ° C for 8 hours (Argon). In this article, the effect of (B) at three wt.% (0.4,0.8,1.2) on the corrosion rate, hardness, and microstructure of alloys was examined. X-ray diffraction (XRD), open circuit potential, electrochemical tests (Tafel extrapolation method), and Macro hardness Brinell were used to study the effect of adding (B) in various amounts to alloys. Saliva was utilized as the corrosion solution for the testing. The inclusion of the alloy element (B) increased hardness and a decrease in particle size, as seen by the microstructures. Furthermore, the corrosion resistance of the master alloy improved next the addition, as shown by Corrosion potential has increased while corrosion current densities have decreased. The corrosion rate for A, A1,A2 and A3 was 14.50, 7.42 , 2.03and 2.77 (mpy) respectively.

Keywords: Powder metallurgy, XRD, Boron addition, Corrosion, Ni-Cr-Mo alloy.

1-Introduction

Nickel-based alloys and cobalt are becoming increasingly used for the manufacture of both removable and fixed dental prostheses. This could be related to the increasing in noble metal costs over the last 30 years, which has been fueled by the rising cost of commodity raw materials(1). Because the oral environment is particularly favorable to corrosion, the dental corrosion process is well recognized to happen in the mouth constantly. Even though the allergenic characteristics of the metal ions in Ni-Cr-based alloys should be carefully evaluated, these alloys are still widely used in dentistry(2). Because of their low cost and good characteristics in veneered restorations, nickel-chromium (Ni-Cr) alloys have been employed for dental prostheses. Because of the probability of allergic reactions to Ni ions, Concerns have been raised about the biocompatibility of Ni-based alloys in an oral environment. The microstructure and characteristics of Ni-based alloys can be altered by adding other elements. Cr is frequently utilized to create a barrier, such that microstructures with a Cr-rich oxide layer keep Ni ions from escaping from



alloys(3). The composition, microstructure, and formation of a passive film layer all influence the corrosion properties of Ni-Cr alloys (4). In polycrystalline alloys, minor elements such as carbon, boron, and zirconium are utilized to strengthen the grain boundary. All of these elements can influence alloy corrosion resistance, at least in principle (18). Experiments found that alloys with 16–27% Cr, 6–17% Mo, and no Be exhibited a low corrosion rate, homogenous protective oxides surface, and a large passivation range (5). Various studies on dental alloys have been discovered through a review of the literature. In acidic artificial saliva, the influence of chemical composition on corrosion of NiCr-based dental casting alloys was investigated by Her-Hsiung Huang (6). The study found that NiCr-based alloys with greater Mo and Cr amounts had a substantially greater passive range on the polarization curve and are resistant to pitting corrosion. Demetrios M. Sarantopoulos et al.(7) corrosion behavior was studied of three novel casting alloys, each of which represents a distinct subclass of casting alloy composition. For corrosion characteristics, new CoPdCr and NiPdCr alloys were examined and compared to current CoCr and NiCr alloys. Palladium addition in NiCr and CoCr alloys did not affect corrosion characteristics, according to the null hypothesis. Using electrochemical methods, Rodrigo Galo et al (8) investigate the influence of the oral environment on dental alloy corrosion of various compositions. The significance of variable component composition in dental alloys was proven in this study. Higher Cr (25 wt%) content in the bulk alloy resulted in better corrosion resistance than lower Cr (12 wt%) concentration. During the research, some variations in microstructure were detected, which altered the corrosion properties of the alloys studied. More Ni ions were released into the media as a result of the lower corrosion resistance, while the amount of Co ions released from the CoCr-Mo dental alloy was modest. Mi-Kyung Han et al. (9) The effect of Zr on the physical characteristics, microstructure, and corrosion resistance of economically pure titanium (cp-Ti) were examined in this work. All Ti-xZr alloys with up to 20% Zr concentration in Ti alloy revealed hcp structures based on optical microscopy and XRD data. The Ti-xZr had a higher hardness than the cp-Ti because of the solid-solution strengthening of α -Ti. The oxidation resistance of Ti-5Zr and Ti-10Zr alloys was greater. The purpose of the study was to use Boron to increase the corrosion resistance of Ni Cr dental alloy.

2- Experimental procedure:-

2.1 Procedure for preparing samples

The method used to prepare the samples is PM, as this process includes several steps:

2.1.1 Preparation of the powders used in the alloy:

The used powders are subjected to several tests to be used in the alloy. One of these tests is particle size analysis. The test was performed for all the alloy components and the added elements (Ni, Cr, Mo, Co, B) by using a laser particle size analyzer and distilled water as a dispersion medium, as shown in Figure (1) and Table (1). The purity of the powders was also checked by using X-ray fluorescent (XRF). The source of these powders (India/CDH fined chemical/Central Drug House (P) Ltd).

Table 1:The powder descriptions.

Powders	Average particle size (μm)	Purity %
Ni	23.53	99.9
Cr	59.03	99.69
Mo	19.76	99.95
Co	18.46	99.6
B	4.931	99.91

Table 2: Alloying element in different percentage

Alloy	Percentage weight	Result alloy wt%
Base alloy Ni-Cr	100%	75 Ni-21Cr- 2Co-2Mo
Ni-Cr/B	0.4%	A-0.4B
Ni-Cr/ B	0.8%	A-0.8B
Ni-Cr/ B	1.2%	A-1.2B

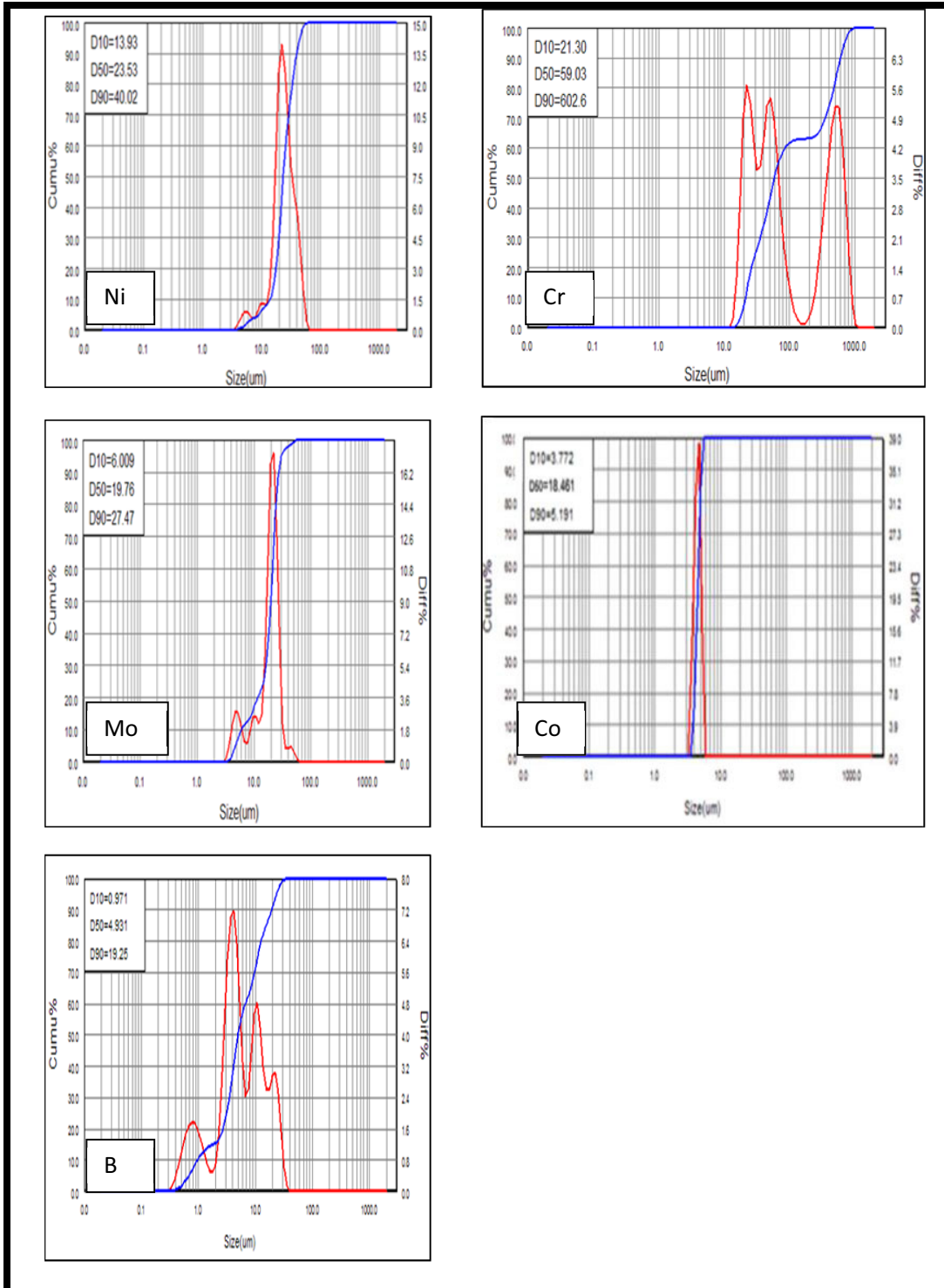


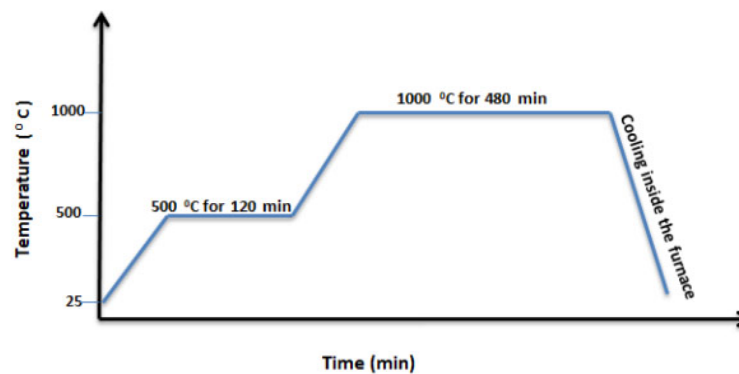
Figure1: Practical size analysis.

2.1.2 Mixing and Compacting powders

The powders are mixed by an electrical rolling mixer type (STGQM-1/5-2) to provide a uniform powder distribution and good mixing of the elements. Steel balls of various sizes (7mm) are used to assure powder mixing, with a little amount of alcohol used to prevent oxidation and friction during mixing. The mixing time is 6 hours. After mixing the powders the blended powder is compacted into green samples with a thickness of 4 mm and a diameter of 13 mm using an electric uniaxial hydraulic press. The die used was a stainless steel single-action die. Graphite was used as a lubricant to reduce friction between the die wall and the punch, as well as between the green compact and the die wall, and to prevent cracks from green compact ejection. For all of the samples, the preferred pressure was determined to be (650MPa).

2.1.3 Sintering process

The green compacts were sintering in an inert high-temperature tube furnace in the presence of an inert gas (Argon). The program of sintering is shown in Figure(2).

**Figure 2:** Sintering program

After sintering, all specimens were grinded using silicon carbide papers of various grits(400,600,800,1000,1200,1500,2000, and 2500). The final stage is to polish with a 15 μm diamond paste and metallographic polishing pads to get a bright mirror finish.

2.2 The samples testes:-

2.2.1-The crystal structures and the phases of the alloys were determined using X-ray diffraction (XRD). The device type (Shimadzu XRD-60000 X-Ray diffractometer) using for analysis.

2.2.2- Optical Microscopy Observation:- After polishing the specimens were etched at room temperature by etching solution (100ml HNO₃, 10ml HF). After that, the specimens were washed and dried with hot air. The microstructure was evaluated by using an optical microscopic.

2.2.3- Electrochemical Tests:-

a- Open Circuit Potential (OCP):

The samples are soaked in artificial saliva during the experiments. The working electrode's potential is calculated concerning the Saturated Calomel electrode (SCE). The working electrode and the reference electrode are both linked to a voltmeter. For each specimen from (0 up to 180)minutes open circuit potential measurements were performed.

b- Potential-dynamic polarization test:

This test has been investigated by Tafel extrapolation type: WENDKING M lap, Germany. Three electrodes were used for the polarization test: Pt electrode (counter electrode) and the saturated Calomel SCE (reference electrode) while the sample (working electrode) according to ASTM G102 (10). Synthetic saliva was used as an electrolyte solution in corrosion studies, table(3) shows its composition, the PH saliva was 5.79 at 37 C⁰ . Potentiodynamic polarization was performed with a scan rate of + 1.0 mV / s and an initiation and end potential of ± 0.250V vs the open circuit potential (Eoc). The following equation can calculate the rate of corrosion :

$$\text{Corrosion rate (mpy)} = 0.13 I_{\text{corr}} (E_w) / A \cdot \rho \dots\dots\dots (3.7)$$

Where:

0.13 = metric and time conversion factor. I corr. = current (μA)

E.W= equivalent weight (g mol⁻¹) ρ: density (g/ cm³)

A= exposed specimen area (cm²) mpy = Corrosion rate (mils penetration per year)

Table 3: Artificial Saliva composition.

No.	Constituent	g/l
1	NaCl	0.4
2	KCl	0.4
3	CaCl ₂ .2H ₂ O	0.906
4	NaH ₂ Po ₄ .2H ₂ O	0.69
5	Na ₂ S.9H ₂ O	0.005
6	Urea	1

2.2.4 Hardness Measurement

Macro hardness Brinell tester was used to determine the hardness of the samples, with an application weight of (31.25)kg/mm² and boll diameter (2.5mm) and an incubation time of (10 seconds) in the state applied weight.

3. Results and Discussion

3.1- XRD Test:

Figure (3) illustrates the XRD pattern for (A) alloy after the sintering process at 1000 C° for 8h under a furnace with an inert gas (Argon). It can be seen from the figure that all elemental Ni, Cr transformed to the present phases. This means that the sintering process period (8hr) was enough to complete the phase transformation process.

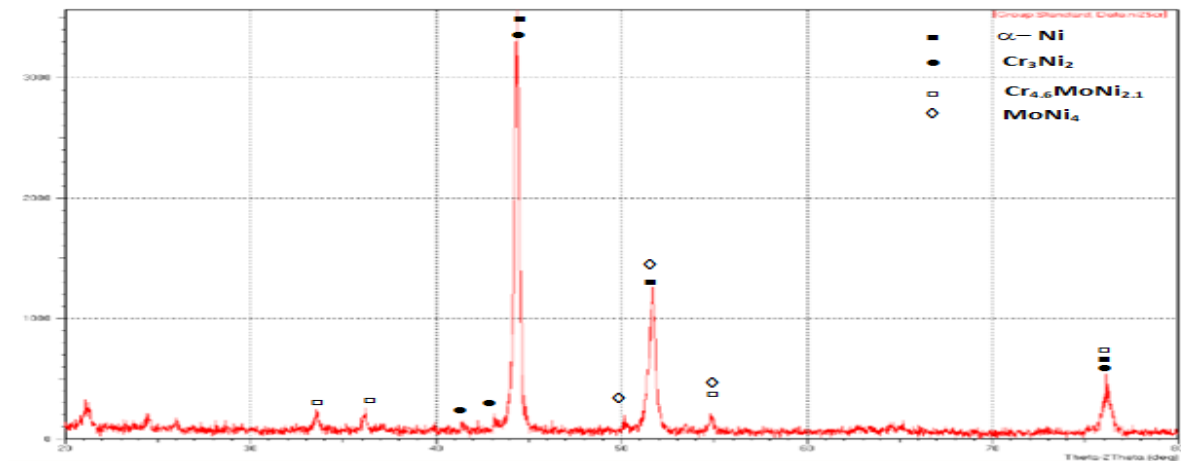


Figure 3: XRD pattern for A alloy after sintering.

3.2-Open Circuit Potential:

Anodic and cathodic reactions occur in any closed electrical circuit. After immersing the sample in corrosive solution, a reaction happened between the corrosive medium and the sample's surface. As a result, a potential known as the "open circuit potential" was created. Because of the potential curve increase and decrease collected over the test time, the building and breakdown of the protective oxide layer were noticed. When the anode reaction(oxidation reaction) equals the cathodic reaction (reduction reaction), the potential value becomes stable (the potential value is set), and the free energy is equal to zero. Figure 4 illustrates the master alloy's open circuit potential with and without three wt% additions (A1, A2, A3). When these additives are applied, the alloy takes on a more noble appearance. The A2 alloy has the lowest possible corrosion value, as seen in Figure 4. The potential for greater negativity as time passes indicates that an inadequate oxide layer has grown to protect the metal from corrosion.

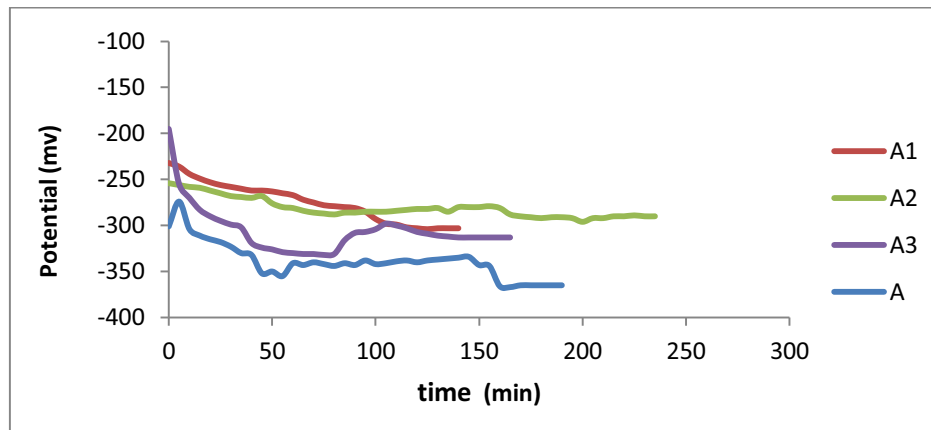


Figure 4: Open circuit potential of alloys in saliva

3.3-Potential-dynamic polarization:

A semi-logarithm chart with anodic and cathodic parts is commonly used to represent the potential-dynamic polarisation curve, which illustrates the electrochemical reactions between the corrosion solution and the sample. This test was done by using the Potentiodynamic polarization test in synthetic saliva for all samples at 37 °C. The corrosion characteristics of the samples (A, A1, A2, and A3) at 37 °C in synthetic saliva solution are depicted by the polarization curves shown in Figure(5). The corrosion parameters (corrosion potential (E_{corr}), Corrosion current density (i_{corr}), and corrosion rate) as a result of a corrosion test for the samples in saliva at 37°C were showed in the table(4). Corrosion of dental alloys is a complicated process that depends not only on the alloy's structure and composition, but also that is influenced by a variety of factors, including surface treatment, environmental conditions around the alloy, and the composition of the surrounding electrolyte used in the study (11). This study illustrated the effect of alloy's composition on corrosion, show that the corrosion rate decrease when adding boron for alloy compared with base alloy(A) this agrees with (12). Boron atoms segregate around the grain boundaries and result in a lowering of the grain boundary energy and inhibition of the nucleation of the second phase, which results in corrosion (13). This effect can be achieved with the use of a very small amount of B. the addition of boron lowers the reactivation rate and corrosion rate and improves intergranular corrosion and the repair capacity of passive films. The alloy with the lowest corrosion rate is (A2) that clearly show in the curves.

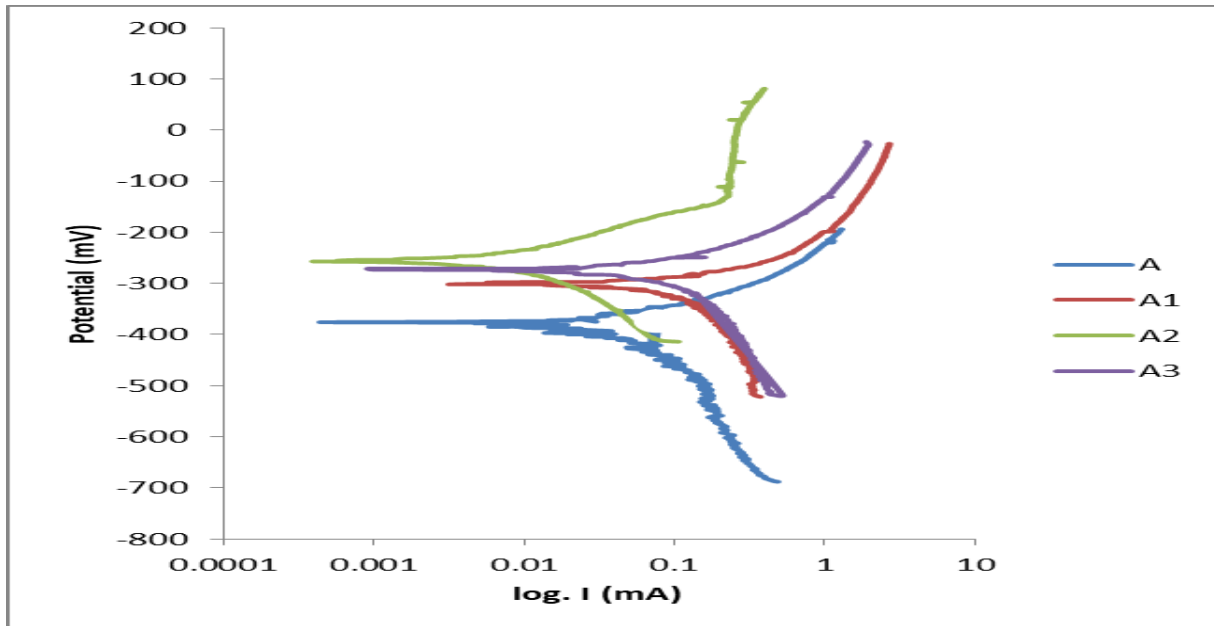


Figure 5: Potential-dynamic polarisation curve for alloys (A, A1, A2, A3) in the saliva solution

Table 4: Illustrate ($I_{corr.}$), (E_{corr}), and Corrosion rates in artificial saliva at 37 C⁰ for all alloys used in this study.

Sample code	$I_{corr.}$ ($\mu A/cm^2$)	$E_{corr.}$ (mV)	Corrosion Rate (mpy)
A	31.72	-366.6	14.50
A1	16.86	-299.4	7.42
A2	4.44	-254.6	2.03
A3	6.97	-273.3	2.77

3.4. Optical Microstructures (OM):

The microstructure of the etched samples was tested using a light optical microscope. The metallography can give a simplified idea about the relationships between the microstructure of the material and the microscopic properties because the size and the shape of grains have a direct effect on the behavior of the material. Figure (6) illustrates the microstructure of etched A, A1, A2, and A3 samples after the sintering process with magnification 400X. The stable precipitates of Ni₂Cr, Cr₃Ni₂ intermetallic, and α -Ni phases are noted in Ni-Cr alloys(14). From the figure, we note the effect of the presence of boron in refining the particle size(15).

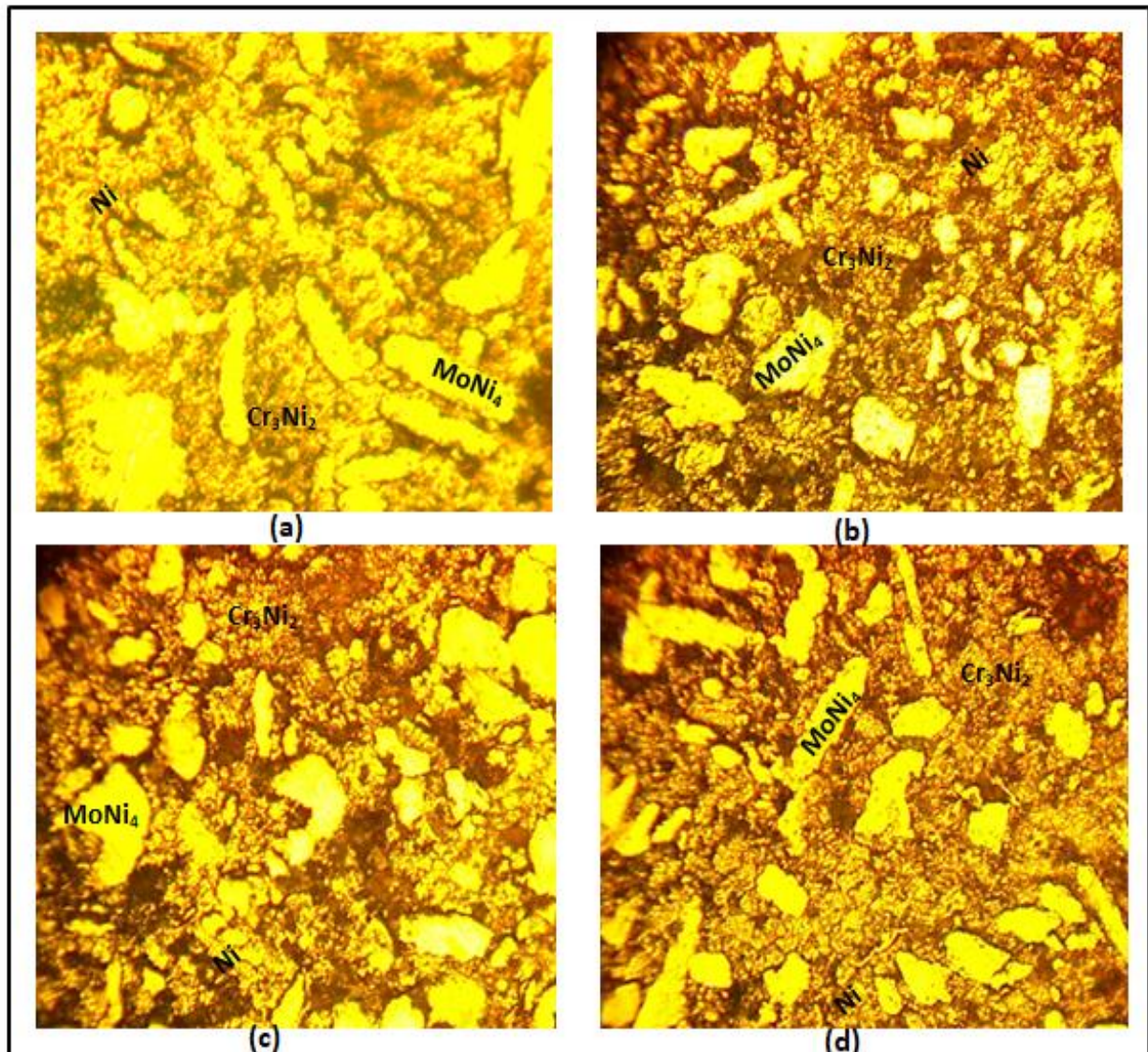


Figure 6: Microstructure for alloy after sintering and etching at 400x(a)A alloy, (b) A₁ alloy,(c)A₂ alloy,(d)A₃ alloy.

3.5-Hardness Test:

The Brinell hardness test was used to determine the hardness of all alloy samples in this study, and the results are shown in figure (7). Each reading represents an average of three readings. As can be seen from the figure (7) Boron additives influence the hardness. A further increase of boron additive also increases the hardness(16). Boron's role in alloy strength is thought to be related to its segregation at grain boundaries. But, Boron additions are higher than the solubility limit caused in the intergranular

precipitation of an M₃B₂ boride, with no further mechanical properties improvement. As a result, it is concluded that Boron is useful as a segregate rather than a precipitate as a strengthening constituent(17).

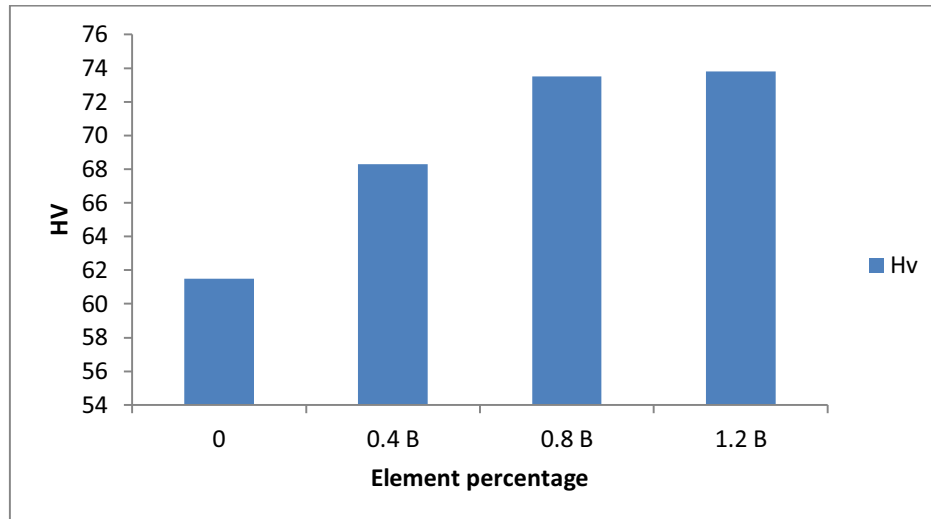


Figure 7: Hardness of A, A1, A2, A3 alloys as a function of B content.

4- Conclusion:-

According to the findings of this study, Through the tests, we notice that the corrosion rate of the base alloy improves when boron is added to the alloy. This effect is due to boron atoms segregate around the grain boundaries and result in a lowering of the grain boundary energy and inhibition of the nucleation of the second phase, which results in corrosion. The best corrosion rate obtained is in alloy A2. The results of the microstructure revealed that adding B to the alloy can reduce grain size. The passive and trans-passive regions' appearance also denoted that the metal had been coated with a protective oxide layer. The hardness of the master alloy was improved by adding B.

5- References:-

[1] Sven Mercieca , Malcolm Caligari Conti , Joseph Buhagiar, Josette Camilleri (*Assessment of corrosion resistance of cast cobalt- and nickel-chromium dental alloys in acidic environments*), Journal of Applied Biomaterials & Functional Materials 2018, Vol. 16(1) 47–54.

[2] Deepti Upadhyay , Manoj A. Panchal , R.S. Dubey , V.K. Srivastava (*Corrosion of alloys used in dentistry: A review*) Materials Science and Engineering A 432 (2006) 1–11.

- [3] Liliana, Porojan, et al. "*Corrosion behavior of Ni-Cr dental casting alloys.*" Int. J. Electrochem. Sci 13 (2018): 410-423.
- [4] Huang, Her-Hsiung. "*Surface characterization of passive film on NiCr-based dental casting alloys.*" Biomaterials 24.9 (2003): 1575-1582.
- [5] Huang, Her-Hsiung. "*Effect of chemical composition on the corrosion behavior of Ni-Cr-Mo dental casting alloys.*" Journal of biomedical materials research 60.3 (2002): 458-465.
- [6] Her-Hsiung Huang (*Surface characterization of passive film on NiCr-based dental casting alloys*), Biomaterials 24 (2003) 1575–1582.
- [7] Demetrios M. Sarantopoulos, DDS, MS, Kelly . Beck, DDS, Robert Holsen, BS, and David W. Berzins, PhD(*Corrosion of CoCr and NiCr dental alloys alloyed with palladium*) The Journal of Prosthetic Dentistry, 2011, Volume 105 Issue 1.
- [8] Rodrigo GALO1 Ricardo Faria RIBEIRO Renata Cristina Silveira RODRIGUES Luís Augusto ROCHA Maria da Glória Chiarello de MATTOS(*Effects of Chemical Composition on the Corrosion of Dental Alloys*), Braz Dent J 23(2) 2012.
- [9] Mi-Kyung Han , Moon-Jin Hwang , Min-Soo Yang , Hong-So Yang , Ho-Jun Song , Yeong-Joon Park(*Effect of Zirconium Content on the Microstructure, Physical Properties and Corrosion Behavior of Ti alloys*), Materials Science & Engineering A, 2014 .
- [10] ASTM, G. 102–89 (Reapproved 1999). Standard Practice for Calculation of Corrosion Rates and Related Information from Electrochemical Measurements.
- [11] Srinivasa B. Rao and Ramesh Chowdhary(*Evaluation on the Corrosion of the Three Ni-Cr Alloys with Different Composition*) ,International Journal of Dentistry, Volume 2011, Article ID 397029, 5 pages.
- [12] Marco A.L. Hernandez-Rodriguez , Dionisio A. Laverde-Cataño , Diego Lozano , Gabriela Martinez-Cazares and Yaneth Bedolla-Gil (*Influence of Boron Addition on the Microstructure and the Corrosion Resistance of CoCrMo Alloy*) Metals 2019, 9, 307.
- [13] Muhammad Saqlain Qurashi1 , Yishi Cui , Jian Wang1, Nan Dong , Jingang Bai1 , Yucheng Wu , Peide Han(*Corrosion Resistance and Passivation Behavior of B-containing S31254 Stainless Steel in a low pH medium*) Int. J. Electrochem. Sci., 14 (2019) 10642 – 10656.
- [14] Ercan Karaköse a , Mustafa Keskin(*Effect of microstructural evolution and elevated temperature on the mechanical properties of Ni–Cr–Mo alloys*) Journal of Alloys and Compounds 619 (2015) 82-90.
- [15] Michael J. Bermingham(*The effect of boron on the refinement of microstructure in cast cobalt alloys*) J. Mater. Res., Vol. 26, No. 7, Apr 14, 2011.
- [16] J. Diabb, A. Juárez-Hernandez, R. Colas, A.G. Castillo, E. García-Sánchez, M.A.L. Hernandez-Rodriguez(*Boron influence on wear resistance in nickel-based alloys*) / Wear 267 (2009) 550–555.
- [17] T.J. GAROSSHEN, T. D. TILLMAN, and G. P. McCARTHY(*Effects of B, C, and Zr on the Structure and Properties of a P/M Nickel Base Superalloy*) metallurgical transactions A, volume 18A, January 1987—69.
- [18] Aleksandra Jalowicka *Effect of Strengthening Additions on the Oxidation and Sulphidation Resistance of Cast Ni-Base Superalloys*, 2013.